Ubiquitous UWB Ranging Error Mitigation With Application to Infrastructure-Free Cooperative Positioning

Maija Mäkelä [ID], Martta-Kaisa Olkkonen [ID], Martti Kirkko-Jaakkola [ID], Toni Hammarberg [ID], Tuomo Malkamäki, Jesperi Rantanen [ID], and Sanna Kaasalainen [ID]

Abstract—**Ultra wideband (UWB) signals are a promising choice for indoor positioning applications, since they are able to penetrate walls to a certain extent. Nevertheless, signal reflections and non-line-of-sight propagation cause bias in the measured range. This ranging error can be corrected with machine learning (ML) methods, such as convolutional neural networks (CNNs). However, these ML models often generalize poorly between different environments. In this work we present an instance-based transfer learning (TL) approach, that enables generalizing a CNN-based ranging error mitigation approach to a new situation with only a few unlabeled training samples. The performance of the UWB error correction approach is demonstrated in a real-life infrastructure-free cooperative positioning setting.**

Index Terms—**Cooperative positioning, infrastructure-free navigation, transfer learning (TL), ultra wideband (UWB).**

I. INTRODUCTION

ULTRA wideband (UWB) positioning has become popular during the recent years. UWB systems transmit extremely short pulses in a way that radio power is spread over the entire spectrum yielding very low power spectral density. UWB operates at frequencies ranging from 3.1 to 10.6 GHz [1]. One of the main benefits of UWB in ranging is that the received power does not undergo fading in multipath environments, such as indoor spaces. Instead, the multipath propagation scenario follows the log-distance law [2]. Thus, UWB is an intriguing choice for a ranging signal in indoor positioning, as it is capable to penetrate walls and other structures. However, when the signal passes through an obstacle [non-line-of-sight (NLOS)], the time-of-arrival (TOA) estimates are distorted. Some problems encountered with UWB pulse propagation are reverberation and multipath cancellation [3]. For instance in in-building UWB pulse reception, the initial line-of-sight (LOS) response is not always the dominant one. Due to multipath effect, there can be several return signals stronger in amplitude than the LOS signal. This results in bias in the measured range, which is problematic from position estimation perspective.

Generally, there are three different options for mitigating the effect of the bias [4]. First option is to discern the NLOS measurements from LOS measurements, and simply exclude the NLOS measurements from position estimation. NLOS detection (as well as mitigation) may be achieved based on statistics derived from channel impulse response (CIR) [5], [6], [7],

[8], [9], [10], or using CIR directly as an input to a neural network [11], [12], [13]. CIR is a representation of the radio environment as received by the UWB sensor [14]. In the analysis, either full channel-state information (CSI) or UWB waveforms can be utilized. Second option is to utilize estimation methods that are robust to outliers in measurements. Robustness may be achieved with certain algorithm choices [15], [16], [17], [18], [19], [20] or combining UWB with other sensors (typically inertial measurements) [21], [22], [23], [24], or both. Third option is to estimate the bias in the UWB measurement, and to remove that before using it in the positioning algorithm. Often NLOS detection and mitigation are treated as separate problems, in which NLOS detection must be solved first [25], [26], [27], [28], [29], but that is not always necessary [30], [31], [32], [33].

Exclusion of the NLOS signals is a suitable approach for computationally constrained devices, that have limited resources for complex bias correction approaches or complicated estimation methods. However, in that case, depending on the environment there may be too few LOS measurements available for positioning. Bias correction approaches make it possible to use all available range measurements. However, they typically require a large amount of training data or characterization of the environment, which makes generalization of the models difficult. Furthermore, especially neural networks using full CIR can require a large number of parameters, which may be problematic in memory constrained devices. Location estimation methods that are robust to NLOS measurements or other outliers may be somewhat computationally complex, but require less information of the navigation environment.

UWB ranging error mitigation approaches do not generalize well from one environment to the other [13], [25]. One potential solution may be transfer learning (TL) [34], a branch of machine learning (ML) research that aims for transferring knowledge from a source domain to a target domain. In the

context of this article, source domain would be the environment or situation where the UWB data has been gathered, and target domain the environment or situation where the knowledge is applied.

To the best of the authors' knowledge, only model-based TL, which aims for adapting an existing trained model to a new target domain, has been applied in UWB localization context. Park et al. [13] applied model-based TL for LOS/NLOS detection. Morawska et al. [35] generate a map of location corrections and utilize model-based TL in generalizing the corrections into new environment. Yin et al. [32] applied TL with shared-hidden-layer autoencoder-type neural network in training a model for ranging error mitigation usable in different environments.

The problem with model-based TL is that it requires labeled samples from the target domain. However, collecting labeled samples is typically time consuming and may not be feasible in all applications. Therefore in this work we apply instance-based TL, which requires only unlabeled samples from the target domain.

Our objective in this work is to find an efficient and generalizable way for correcting the bias in UWB ranging. The proposed method will be demonstrated in practice in a infrastructure-free cooperative positioning scenario. In tactical and rescue operations the location of the team members is a critical part of situational awareness. However, in such situations localization methods based on external infrastructure (for example, Global Navigation Satellite Systems) may not be available. Infrastructure-free navigation methods, that are based on carry-on sensors, such as inertial measurement units (IMUs), enable standalone position estimation with self-contained systems [36], [37], [38]. The positioning performance may be enhanced with cooperative approaches, where the team members measure distances to one another [37], [39]. UWB signal is well suited to this purpose.

The main contributions of this work are as follows.

1) We propose a CNN-based method for estimating the bias caused by NLOS and multipath conditions to UWB range measurements. The method does not require explicit knowledge of the LOS/NLOS status.
2) We show an effective TL approach for overcoming the problem of poor generalization of ML models between environments. Contrary to existing research, TL is achieved without labeled samples from the target environment.
3) We demonstrate the effect of different ranging error mitigation approaches on cooperative infrastructure-free positioning in a real world measurement campaign.

The rest of this article is organized as follows. Section II gives an overview of instance-based TL. Section III summarizes the methods used in this work and Section IV discusses the tests and test results. Finally, Section V concludes this article and discusses future research on this topic.

II. INSTANCE-BASED TL

This section gives an overview of *instance-based noninductive TL*. The derivation is done following Yang et al. [34].

A. Problem Formulation

In instance-based TL the objective is to use labeled data from a source domain to accomplish a task in target domain. Formally, a feature space $\mathcal{X}$ and marginal probability distribution $\mathbb{P}^X = P(\mathbf{x}|\mathbf{x} \in \mathcal{X})$ together form a *domain* $\mathbb{D}$. A *task* contains a label space $\mathcal{Y}$ and predictive function $f(\mathbf{x})$. In probabilistic terms, $f(\mathbf{x})$ may be expressed as $\mathbb{P}^{Y|X} = P(y|\mathbf{x} \in \mathcal{X})$.

Source domain is then $\mathbb{D}_S = \{\mathcal{X}_S, \mathbb{P}_S^X\}$ and similarly *target domain* is $\mathbb{D}_T = \{\mathcal{X}_T, \mathbb{P}_T^X\}$. *Source domain labeled data* are noted as $\mathcal{D}_S = \{(\mathbf{x}_{S_i}, y_{S_i})\}_{i=1}^{n_S}$, where $\mathbf{x}_{S_i} \in \mathcal{X}_S$ and $y_{S_i} \in \mathcal{Y}_S$. Similarly *target domain unlabeled data* are $\mathcal{D}_T = \{(\mathbf{x}_{T_i})\}_{i=1}^{n_T}$ with $\mathbf{x}_{T_i} \in \mathcal{X}_T$. The number of instances in source and target domains are n_S and n_T, respectively. The goal of TL is to learn the target domain task $\mathbb{T}_T = \{\mathcal{Y}_T, f_T(\cdot)\}$.

B. Instance-Based Noninductive TL

In instance-based noninductive TL it is assumed that the difference between source domain $\mathbb{D}_S$ and target domain $\mathbb{D}_T$ results only from the difference between the marginal distributions, formally $\mathbb{P}_S^X \neq \mathbb{P}_T^X$. Notably, it is assumed that $\mathbb{P}_S^{Y|X} = \mathbb{P}_T^{Y|X}$. Now the objective is to learn the target domain task $\mathbb{T}_T$, specifically the task predictive function $f_T(\cdot)$ in terms of its parameters θ_T. The optimal solution can be achieved by solving the optimization problem

$$\theta_T^* = \arg \min_{\theta_T \in \Theta} \mathbb{E}_{(\mathbf{x},y) \sim \mathbb{P}_T^{X,Y}} [\ell(\mathbf{x}, y, \theta_T)] \tag{1}$$

where $\ell(\mathbf{x}, y, \theta_T)$ is loss function in terms of parameters θ_T. Without target domain labeled data the optimization problem in (1) cannot be solved directly. With Bayes' rule and definition of expectation it can be shown that (1) becomes

$$\theta_T^* = \arg \min_{\theta_T \in \Theta} \mathbb{E}_{(\mathbf{x},y) \sim \mathbb{P}_S^{X,Y}} \left[\frac{P_T(\mathbf{x},y)}{P_S(\mathbf{x},y)} \ell(\mathbf{x}, y, \theta_T)] \right]. \tag{2}$$

Using the assumption $\mathbb{P}_S^{Y|X} = \mathbb{P}_T^{Y|X}$, the likelihood ratio in (2) becomes

$$\frac{P_T(\mathbf{x},y)}{P_S(\mathbf{x},y)} = \frac{P_T(y|\mathbf{x})P_T(\mathbf{x})}{P_S(y|\mathbf{x})P_S(\mathbf{x})} = \frac{P_T(\mathbf{x})}{P_S(\mathbf{x})}.$$

Now the optimization problem in (2) can be solved without label information using the empirical approximation

$$\theta_T^* = \arg \min_{\theta_T \in \Theta} \sum_{i=1}^{n_S} \frac{P_T(\mathbf{x}_{S_i})}{P_S(\mathbf{x}_{S_i})} \ell(\mathbf{x}_{S_i}, y_{S_i}, \theta_T). \tag{3}$$

The density ratio $\frac{P_T(\mathbf{x})}{P_S(\mathbf{x})}$ can be estimated with a rejection sampling based approach, for example [40]. Other potential approaches include function approximation and Kernel mean matching [34].

In rejection sampling a binary random variable $\delta \in \{0, 1\}$ is utilized as a selection variable such that $\delta = 0$ denotes the target distribution P_T and $\delta = 1$ the source distribution P_S. Using this notation the target marginal distribution can be expressed as
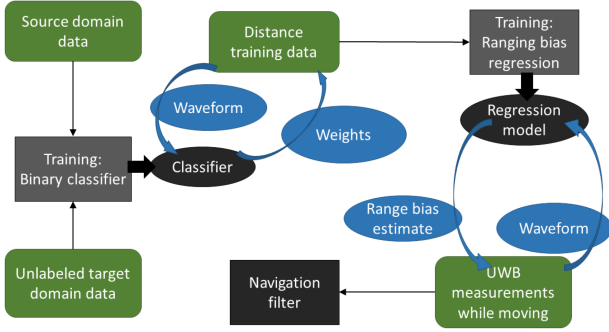
Fig. 1. Illustration of the instance-based TL process for UWB ranging error mitigation.

Fig. 2. Examples of received UWB waveforms in different environments. The transmitted pulse is shown in green.

$P_T(\mathbf{x}) = P(\mathbf{x}|\delta = 0)$, and similarly source marginal distribution $P_S(\mathbf{x}) = P(\mathbf{x}|\delta = 1)$. Now based on Bayes' rule

$$
\begin{aligned}
\frac{P_T(\mathbf{x})}{P_S(\mathbf{x})} &= \frac{P(\mathbf{x}|\delta = 0)}{P(\mathbf{x}|\delta = 1)} \\
&= \frac{\frac{P(\delta=0|\mathbf{x})P(\mathbf{x})}{P(\delta=0)}}{\frac{P(\delta=1|\mathbf{x})P(\mathbf{x})}{P(\delta=1)}} = \frac{P(\delta = 1)P(\delta = 0|\mathbf{x})}{P(\delta = 0)P(\delta = 1|\mathbf{x})} \\
&= \frac{P(\delta = 1)(1 - P(\delta = 1|\mathbf{x}))}{P(\delta = 0)P(\delta = 1|\mathbf{x})} \\
&= \frac{P(\delta = 1)}{P(\delta = 0)} \left(\frac{1}{P(\delta = 1|\mathbf{x})} - 1 \right).
\end{aligned} \tag{4}
$$

Thus, the density ratio can be estimated as $\frac{P_T(\mathbf{x}_{S_i})}{P_S(\mathbf{x}_{S_i})} \propto \frac{1}{P(\delta=1|\mathbf{x}_{S_i})}$. A binary classifier, that distinguishes between the source and target domain instances, can be used to estimate probability $P(\delta = 1|\mathbf{x}_{S_i})$. The density ratio estimates can be used for reweighting the source domain instances or for importance sampling. In this work we use reweighting.

III. METHODS

This section summarizes the details of applying TL for UWB ranging error mitigation in infrastructure-free pedestrian navigation. The process is illustrated in Fig. 1.

A. UWB Signals

We can describe CIR of an UWB system by the general equation for impulse response $h(t)$ of a fading multipath channel

$$
h(t) = \sum_{N}^{i=0} a_i \delta_0(t - \tau_i). \tag{5}
$$

The $h(t)$ in (5) depicts the signal propagation paths N in a reflective environment between the transmitter and receiver [1]. Attenuation between the transmitter and receiver on path i is denoted by a_i and propagation delay at time t by τ_i, and δ_0 is the Dirac delta function
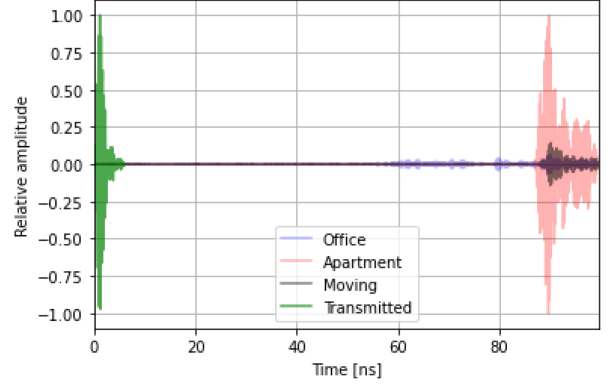
$$
y(t) = x(t) * h(t) + n(t). \tag{6}
$$

If $x(t)$ is the UWB pulse sent by the transmitter, the total received signal in (6) is a superposition of the received signal echoes. Convolution is denoted by $*$.

Additive white Gaussian noise $n(t)$ accounts for noise components other than those on the propagation path, such as sensor noise. In this work we use the received signal $y(t)$ as an input for the neural network. In case where all transmitters are of same type, i.e., transmit the same signal $x(t)$, deconvolution of the signal to obtain CIR may be omitted to preserve computational power. However, if a mixture of different transmitters is used, the method proposed in this article may be applied also to the CIR. Example of received UWB waveforms in different environments is shown in Fig. 2.

B. Transfer Learning

Both UWB waveforms and CSI derived from CIR have already been applied as CNN input for environment recognition [41], [42]. These works show that environments can be differentiated based on the UWB waveform or CIR. Thus, it is justified to use a similar approach for training the binary classifier, that in instance-based TL estimates the probability $P(\delta = 1|\mathbf{x}_{S_i})$. In this work we apply convolutional neural networks (CNNs) for both instance weighting and regression tasks [43]. CNNs learn convolutional kernels during training process, and thus are well suited for images and other spatially dependent data. They usually have fewer parameters compared to fully connected neural networks. For weighting the distance training samples, we first train a simple CNN for binary classification between the static distance measurements (source domain) and the measurements made while moving (target domain). The CNN hyperparameters, that were chosen experimentally, are listed in Table I. Explanation of the different terms may be found from [43], for example. The weights used in instance-based TL will be computed based on the neural network output corresponding to the source domain class.

C. Ranging Error Mitigation

We train another CNN for estimating the bias in the UWB range measurement. The training target is the measurement bias, more precisely the difference between the distance reported by

TABLE I
NEURAL NETWORK HYPERPARAMETERS

	Weighting CNN	Bias estimation CNN
Input	UWB waveform	UWB waveform
Convolutional layers	1	3
Convolution kernel size	9	9
MaxPooling size	4	5
Fully connected layer neurons	None	512, 256, 128, 128, 128
Activation function	Hyperbolic tangent	Hyperbolic tangent
Output layer	2 neurons, Softmax	1 neuron, Linear
Output	Source and target domain probability	UWB ranging bias
Optimizer	Adam	Adam
Loss Function	Binary Crossentropy	Mean Squared Error
Initial learning rate	10^{-3}	10^{-5}
Learning rate drop	15 epochs	10 epochs
Early stopping	30 epochs	32 epochs

the radio and the true distance between the radios. For this task we need a more complex CNN, which hyperparameters are listed in Table I.

In instance-based TL the loss of each individual sample will be weighted according to (3). Those source domain training samples that are more similar to the target domain, will have a larger effect when updating the neural network weights. However, in practice the weights are often unevenly distributed such that a small number of the sample weights have a very large value, whereas the rest are relatively small. In this case instance-based TL approaches may yield poor results despite theoretically correct weighting [44]. As a practical observation, for example neural network optimizers perform better with roughly evenly distributed weights.

For this reason we transform the weights before using them in training. First, we apply hyperbolic tangent, which is a sigmoid-type function, to spread the weights more evenly. The resulting values range from -1 to 1, so we scale the values back to the original range such that the minimum and maximum weight remain the same. This way the relative order of the weights and the scale of the values are preserved, and the CNN training works better.

D. Infrastructure-Free Cooperative Positioning

IMUs measure acceleration and rotation, and can provide relative localization independent of any external signals. The IMU may be mounted on the body or on the foot of a pedestrian. While walking or running, the foot of the pedestrian will be momentarily stationary at each step. When placing the IMU on the pedestrians foot, this fact can be utilized to reduce the heading drift by applying Zero-Velocity Updates (ZUPTs) in the navigation filter [45]. This is called footmounted pedestrian dead reckoning (PDR) [46].

In this work, we combine an independent PDR position solution with cooperative UWB ranging for a team of two pedestrians. This is done using an extended Kalman filter (EKF) [47], which processes PDR-based location increments aiming to compensate for heading drift typical for inertial navigation. The EKF is fully decentralized, meaning that the position solutions

of the team members are computed independent of each other. The state is modeled as $\mathbf{m} = [x\ y\ z\ \theta]^T$, where x, y, and z are the 3-D coordinates and θ is the heading offset. The state and measurement model, $\mathbf{f}$ and $\mathbf{h}$, respectively, are similar to our previous publication [48]. State model is

$$\mathbf{f}(\mathbf{m}_{t-1}) = \mathbf{m}_{t-1} + \begin{bmatrix} R(\theta_{t-1})\mathbf{x}_{incr,t} \\ 0 \end{bmatrix} \qquad (7)$$

where $\mathbf{x}_{incr}$ denotes the difference between consecutive PDR location estimates and $R(\theta)$ is a rotation matrix on xy-plane. The measurement model is

$$\mathbf{h}(\mathbf{m}_t) = \left\| \begin{bmatrix} x_t \\ y_t \\ z_t \end{bmatrix} - \mathbf{x}_{col} \right\| = r_{\text{UWB},t} \qquad (8)$$

where $r_{\text{UWB},t}$ refers to the range measurement. To account for the uncertainty in the location of the collaborating team member, $\mathbf{x}_{col}$, their location uncertainty is scaled along the direct line between the location estimates using $\sigma^2_{\text{col},t} = \mathbf{u}_t^T \text{cov}(\mathbf{x}_{col})\mathbf{u}_t$, where $\mathbf{u}_t$ is the unit vector pointing from one team member to the other [49]. Noise term $\sigma^2_{\text{col},t}$ is then added to the measurement covariance at each update. The team members location and location uncertainty are assumed to be transmitted alongside the ranging signal.

IV. TESTS AND TEST RESULTS

This section describes the tests and summarizes the test results in order to verify the presented approach.

A. Data Collection

The UWB devices used in this work are TimeDomain PulsOn 440 radios (P440), which have been used both in ranging data collection and navigation tests. The collected waveforms consists of 1632 datapoints depicting the magnitude of the received UWB pulse. The radios report also the two-way TOA-based range measurement.

1) Range Data Collection: The training data for ranging error mitigation has been collected at two different locations. First environment is Finnish Geospatial Research Institute's (FGI) former office in Kirkkonummi, Finland, consisting of regular office rooms and hallways in three floors. Second data collection site is a regular apartment in a multifloor apartment building.

At FGI office there are several reference points marked on floor that have been located precisely with a total station. At the apartment a grid of reference points at $0.5\,\text{m} \times 0.5\,\text{m}$ was measured and marked on the floor. The UWB radios were placed on a number of distinct reference points with a known distance between them. The training data contains both LOS and NLOS measurements.

At the office a total of $166\,700$, and at the apartment total of $170\,681$ training samples was collected. A histogram of the different reference distances is shown in Fig. 3, and the histogram of the residual ranging errors (for part of the data) in Fig. 4.
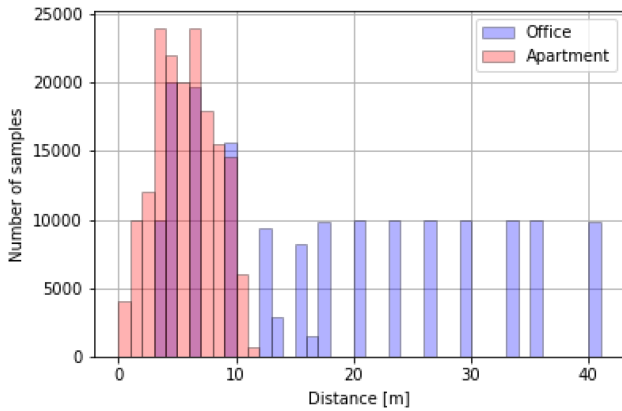
Fig. 3. Number of measured training data at different distances in office and apartment environments.
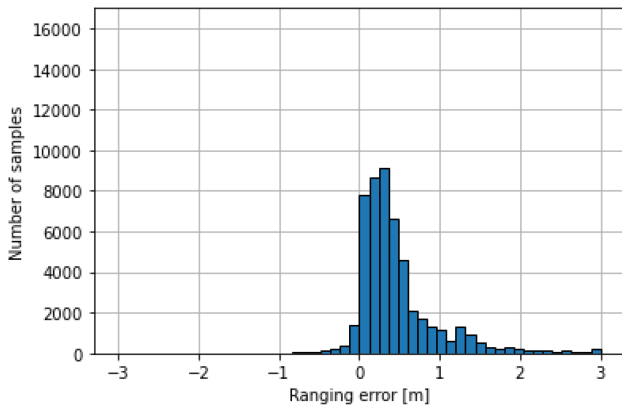

Fig. 5. Distribution of residual ranging errors after correction using model trained without TL. Calculated for independent test set not used during CNN training.

Fig. 4. Distribution of ranging errors without correction.

Fig. 6. Distribution of residual ranging errors after correction using model trained with TL. Calculated for independent test set not used during CNN training.

2) Navigation Test Setup: In navigation test there are two persons operating as a team. Both are equipped with the P440 radios carried approximately at shoulder level. For footmounted PDR wireless XSens Awinda IMUs are placed on the foot of each team member. The reference system is carried by one of the pedestrians, and consists of NovAtel Propak6 receiver and Honeywell HG1700-AG58 IMU mounted on a backpack with metal frame.

The navigation test was conducted at FGI, where also part of the ranging data has been collected. The pedestrians start the route from outdoors, enter the building at ground level (approximately at $(-19, 38)$ in Figs. 8–10) and climb stairs to the third floor. At third floor they visit few office rooms before exiting the building again at ground level through different doors and returning to the starting point.

B. Ranging Error Mitigation

For determining the appropriate weights for the collected source domain data samples, we train a binary CNN classifier as explained in Section III. We use Python and Tensorflow for training all neural networks. As target domain samples, we use all of the range measurements obtained during the navigation test, 631 in total. Since the amount of source domain samples, 337 381, is considerably larger than target domain samples, the training data needs to be balanced. We randomly choose
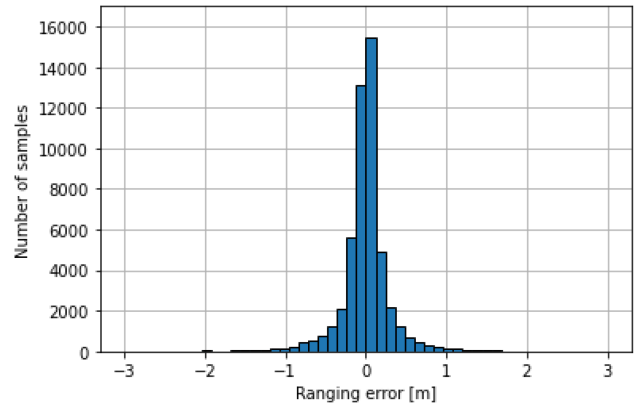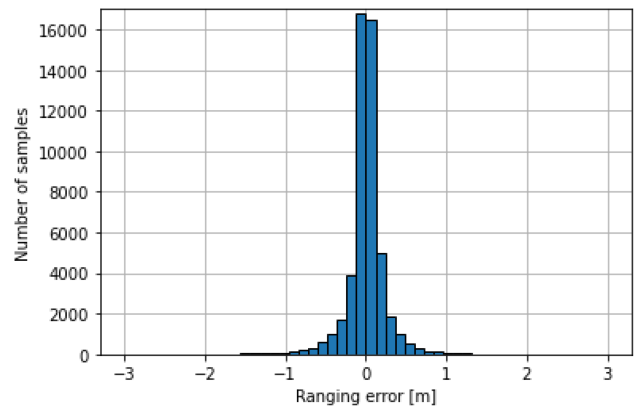
a number of samples matching the amount from navigation tests from both office and apartment environments, so the total amount of training data for the classifier is 1893 samples. We use randomly chosen 20 % of those samples as validation set during training. With this classifier, 94.8 % of all available 337 381 source domain samples would have been correctly classified.

In order to compare the effect of ranging error mitigation with and without instance-based TL, we train two CNNs. The structure and other training conditions of both neural networks are the same as detailed in Table I. We randomly choose 80 % of the training samples for training the neural network, 5% for validation during the training phase, and 15% as separate test set.

The residual ranging errors of the test set are shown in Fig. 5 for unweighted CNN and in Fig. 6 for weighted CNN. We can see that the distribution of residual ranging error for the weighted and unweighted CNNs are very close to each other, even though for weighted case the standard deviation is slightly smaller. The numerical values are given in Table II. However, it should be noted that these results do not directly correspond to the target domain case where we do not have reference for the distance measurements. From target domain, Fig. 7 shows the estimated range biases for the two different CNNs. The unweighted CNN

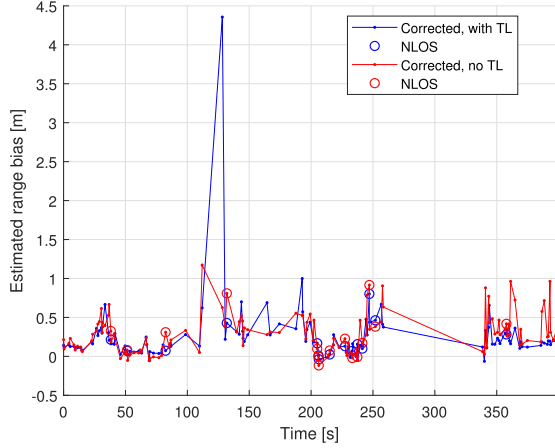| [m]	Uncorr. range	CNN, no TL	CNN, TL
μ	0.45	0.00	0.00
σ^2	0.25	0.07	0.07

Fig. 7.   Estimated range biases for Person 1 with and without TL. NLOS measurements are reported by the P440 UWB radio.

marked in red makes somewhat larger corrections especially at the end of the test, where the team members are outdoors.

C. Navigation Results

Indoors, it is near impossible to obtain a reliable reference of the distance between two UWB radios while they are carried by pedestrians moving at a fast pace. Therefore, we evaluate the performance of instance-based TL via positioning accuracy in realistic navigation test. The proposed approach is evaluated against uncorrected UWB ranges, uncorrected UWB ranges with NLOS exclusion (based on inbuildt detection method of the P440 device), uncorrected UWB ranges combined with normalized EKF innovation-based outlier test [50], and CNN-based correction that has been trained without instance weighting.

In order to isolate the effect of ranging error mitigation from other design choices, certain simplifications have been made. The heading estimate has been artificially initialized to the heading matching the reference solution at the beginning of the test. Poor initialization of the heading would affect navigation performance considerably during such a short test taking only 6 min. However, determining an initialization procedure is beyond the scope of this work. For UWB measurements, in EKF we use the mean and covariance values presented in Table II for each test case.

During the test only Person 2 carries the reference system that enables computing positioning errors throughout the whole test. Nevertheless, utilizing the fact that both team members start and end the test at the same position, we can compute the so called loop closure error. It represents the difference between the expected and estimated location at the end of the test.

The standalone PDR solutions are illustrated in Fig. 8, and the positioning errors are given in Table III for Person 1 and
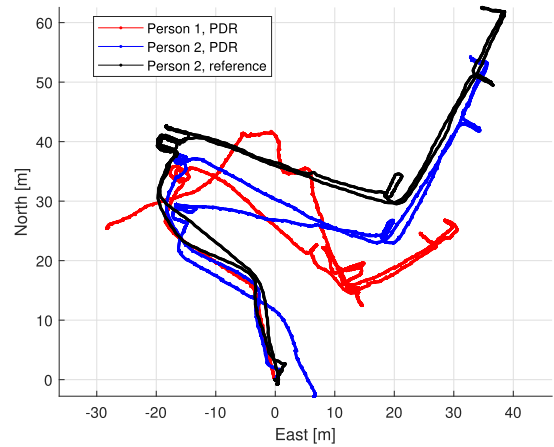

Fig. 8.   Standalone PDR results for Person 1 and Person 2.

TABLE III
LOOP CLOSURE ERROR FOR PERSON 1

Error [m]	PDR only	Uncorr.	Uncorr., no NLOS	Uncorr., innov. test	CNN, no TL	CNN, TL
Loop closure	38.61	9.36	14.42	15.58	18.15	13.70
Loop closure XY	38.02	3.46	11.41	13.33	16.23	11.04
Loop closure Z	6.72	8.62	8.75	8.00	8.09	8.04

TABLE IV
POSITIONING ERRORS FOR PERSON 2

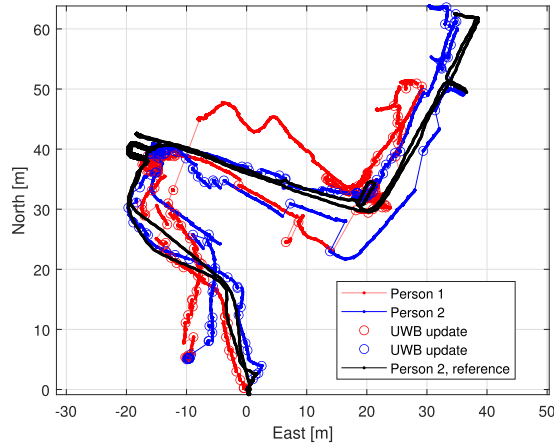| Error [m]	PDR only	Uncorr.	Uncorr., no NLOS	Uncorr., innov. test	CNN, no TL	CNN, TL
Avg.	8.90	6.20	7.94	7.21	6.44	5.86
Avg. XY	7.14	4.35	6.57	5.46	4.90	3.87
Avg. Z	4.45	3.84	3.91	4.33	3.88	3.91
Loop closure	15.10	11.90	16.22	20.12	19.41	15.44
Loop closure XY	7.07	3.57	11.48	15.44	16.06	10.84
Loop closure Z	13.34	11.35	11.46	12.88	10.88	10.97

Fig. 9.   Cooperative navigation solution for both team members.

in Table IV for Person 2 carrying the reference. From the illustrations it can be seen that the heading of the PDR solutions drifts considerably.

Fig. 9 shows the cooperative positioning results when TL-based UWB ranging error mitigation has been applied. It can be seen from the figure, as well as from Tables III and IV,
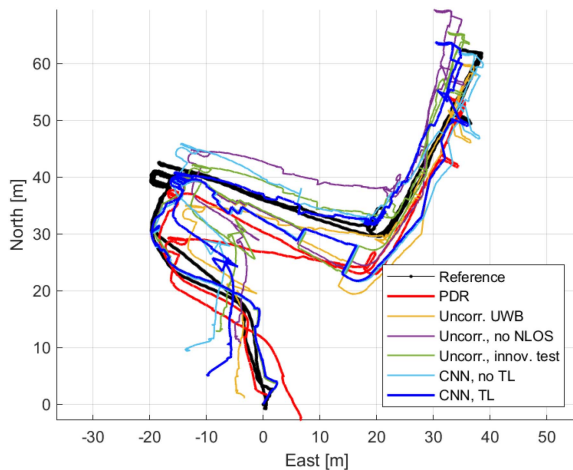
Fig. 10. Navigation results with different methods for Person 2.

that especially in horizontal plane the error has been reduced considerably.

Fig. 10 shows the results for Person 2 with standalone PDR and the different ranging options. Based on the illustration, as well as the numerical results in Tables III and IV it is plain that the TL-based ranging error mitigation yields the best performance. However, in vertical direction the improvement is not as evident. Nevertheless, the results show that correcting the ranges with poorly adapted CNN may even degrade the positioning performance compared with the uncorrected case. In addition, excluding NLOS measurements (15 out of 132 for Person 1 and 5 out of 146 for Person 2) or outliers based on EKF innovation (18 for Person 1 and 23 for Person 2) seems to degrade the navigation performance. This is related to the Kalman filter state formulation. If the heading offset estimate has not converged, in absence of measurements the PDR-based track continues to wrong direction.

In terms of loop closure error the uncorrected case yields numerically best results. This is due to a sudden jump in the position estimates toward the end of the track, shown in Fig. 10 approximately at $(-5, 25)$, resulting from the other team member emerging from inside the building after a pause in UWB measurement updates. Considering the positioning errors for the whole track in Table IV, the loop closure result for the uncorrected case seems somewhat coincidental. Out of the different mitigation approaches, the TL-based corrections yield best loop closure errors for both team members.

D. Discussion

We have shown that the UWB ranging error can be mitigated with a CNN-based approach. Compared with uncorrected ranging error, both CNN approaches yield close to zero-mean residual error distribution. Furthermore, the distributions are not skewed or strongly heavytailed. This is beneficial especially from Kalman filtering point of view. The distributions from CNNs trained with and without TL are relatively close to each other. However, there is a difference resulting from how individual samples are corrected. The results show that without TL the

CNN tends to apply larger corrections. From practical point of view, direct evaluation of the error mitigation performance is not possible for pedestrians moving indoors at fast pace. Therefore, we evaluate the performance through positioning results.

The navigation test results show that TL-based UWB ranging error mitigation performs best compared with uncorrected ranging or even using corrected ranges without adaptation to the situation and environment. The performance improvements are especially evident in horizontal direction, whereas in vertical direction there is little to no improvement. The poor navigation accuracy in vertical direction is typical to PDR, where the height solution generally tends to drift upward. Including other sensors to the fusion, such as barometer, enables more accurate height estimation [22], [51].

The obvious drawback of the presented approach is having to train several neural networks. This might not be feasible in tactical operations. Initializing the network with pretrained weights may speed up the training process. Nevertheless, for the weight generation in instance-based TL only a few, notably unlabeled, samples are needed. For model-based TL applied in existing research (discussed in Section I) labeled samples are a necessity, which makes model-based TL even less applicable in tactical scenarios. It is expected that the progress in CPU and GPU development, as well as in quantum computing, will make training the networks sufficiently fast even for tactical and rescue missions.

V. Conclusions and Future Work

In this work, we have demonstrated an instance-based TL approach that solves the problem of poor generalization of ML models over different environments in indoor navigation. The CNN-based approach corrects UWB ranging errors, and is easily generalized to different environments and situations with only a small number of unlabeled training samples. The performance of the presented approach is validated in real-world infrastructure-free cooperative positioning test. In addition to cooperative localization, this UWB ranging error mitigation method is well suitable also to other applications besides sensor-based navigation.

Future work will include computationally efficient methods for CNN training and means for mitigating the effect of correlated estimation errors in cooperative positioning.

References

[1] D. Porcino, J. Sachs, and R. Zetik, "UWB Ranging," in *UWB Communication Systems a Comprehensive Overview*, M. G. d. Benedetto, T. Kaiser, and A. Molisch, Eds. New York, NY, USA: Hindawi Publishing Corporation, 2006, pp. 411–446.

[2] C. Sturm, U. J. Monich, T. Zwick, W. Wiesbeck, and H. Boche, "An empirical approach to the prediction of the channel capacity in ultra wideband indoor propagation channels," in *Proc. IEEE Antennas Propag. Soc. Int. Symp.*, 2008, pp. 1–4.

[3] P. D. Smith, S. R. Cloude, and R. J. Fontana, "Experimental results from an ultra wideband precision geolocation system," *Ultra-Wideband, Short-Pulse Electromagn.*, vol. 5, pp. 215–223, 2002.

[4] J. Khodjaev, Y. Park, and A. S. Malik, "Survey of NLOS identification and error mitigation problems in UWB-based positioning algorithms for dense environments," *Ann. Telecommun. - Annales des Télécommun.*, vol. 65, no. 5, pp. 301–311, Jun. 2010.

[5] Y. Wang, K. Gu, Y. Wu, W. Dai, and Y. Shen, "NLOS effect mitigation via spatial geometry exploitation in cooperative localization," *IEEE Trans. Wireless Commun.*, vol. 19, no. 9, pp. 6037–6049, Sep. 2020.

[6] A. Musa, G. D. Nugraha, H. Han, D. Choi, S. Seo, and J. Kim, "A decision tree-based NLOS detection method for the UWB indoor location tracking accuracy improvement," *Int. J. Commun. Syst.*, vol. 32, no. 13, 2019, Art. no. e3997.

[7] Z. Zeng, S. Liu, and L. Wang, "UWB NLOS identification with feature combination selection based on genetic algorithm," in *Proc. IEEE Int. Conf. Consum. Electron.*, 2019, pp. 1–5.

[8] N. Decarli, D. Dardari, S. Gezici, and A. A. D'Amico, "LOS/NLOS detection for UWB signals: A comparative study using experimental data," in *Proc. IEEE 5th Int. Symp. Wireless Pervasive Comput.* 2010, pp. 169–173.

[9] K. Gururaj, A. K. Rajendra, Y. Song, C. L. Law, and G. Cai, "Real-time identification of NLOS range measurements for enhanced UWB localization," in *Proc. Int. Conf. Indoor Positioning Indoor Navigation*, 2017, pp. 1–7.

[10] V. Barral, C. J. Escudero, and J. A. García-Naya, "NLOS classification based on RSS and ranging statistics obtained from low-cost UWB devices," in *Proc. 27th Eur. Signal Process. Conf.*, 2019, pp. 1–5.

[11] C. Jiang, J. Shen, S. Chen, Y. Chen, D. Liu, and Y. Bo, "UWB NLOS/LOS classification using deep learning method," *IEEE Commun. Lett.*, vol. 24, no. 10, pp. 2226–2230, Oct. 2020.

[12] M. Stahlke, S. Kram, C. Mutschler, and T. Mahr, "NLOS detection using UWB channel impulse responses and convolutional neural networks," in *Proc. Int. Conf. Localization GNSS*, 2020, pp. 1–6.

[13] J. Park, S. Nam, H. Choi, Y. Ko, and Y.-B. Ko, "Improving deep learning-based UWB LOS/NLOS identification with transfer learning: An empirical approach," *Electronicsweek*, vol. 9, no. 10, Oct. 2020, Art. no. 1714.

[14] M. Cimdins, S. O. Schmidt, and H. Hellbrück, "Comparison of I/Q-and magnitude-based UWB channel impulse responses for device-free localization," in *Proc. IEEE Int. Conf. Localization GNSS*, 2021, pp. 1–7.

[15] İ. Güvenç, C.-C. Chong, F. Watanabe, and H. Inamura, "NLOS identification and weighted least-squares localization for UWB systems using multipath channel statistics," *EURASIP J. Adv. Signal Process.*, vol. 2008, no. 1, Dec. 2007, Art. no. 271984.

[16] X. Li, Y. Wang, and K. Khoshelham, "Comparative analysis of robust extended Kalman filter and incremental smoothing for UWB/PDR fusion positioning in NLOS environments," *Acta Geodaetica et Geophysica*, vol. 54, no. 2, pp. 157–179, Jun. 2019.

[17] T. Liu, G. Li, G. Lu, S. Li, and S. Tian, "Robust hybrid cooperative positioning via a modified distributed projection-based method," *IEEE Trans. Wireless Commun.*, vol. 19, no. 5, pp. 3003–3018, May 2020.

[18] C.-H. Park and J.-H. Chang, "Robust localization based on ML-Type, multi-stage ML-Type, and extrapolated single propagation UKF methods under mixed LOS/NLOS conditions," *IEEE Trans. Wireless Commun.*, vol. 19, no. 9, pp. 5819–5832, Sep. 2020.

[19] P. Müller, H. Wymeersch, and R. Piché, "UWB positioning with generalized Gaussian mixture filters," *IEEE Trans. Mobile Comput.*, vol. 13, no. 10, pp. 2406–2414, Oct. 2014.

[20] H. Nurminen, T. Ardeshiri, R. Piché, and F. Gustafsson, "A NLOS-robust TOA positioning filter based on a skew-t measurement noise model," in *Proc. IEEE Int. Conf. Indoor Positioning Indoor Navigation*, 2015, pp. 1–7.

[21] D.-H. Kim and J.-Y. Pyun, "NLOS identification based UWB and PDR hybrid positioning system," *IEEE Access*, vol. 9, pp. 102917–102929, 2021.

[22] M. Mäkelä, M. Kirkko-Jaakkola, J. Rantanen, and L. Ruotsalainen, "Proof of concept tests on cooperative tactical pedestrian indoor navigation," in *Proc. IEEE 21st Int. Conf. Inf. Fusion*, 2018, pp. 1369–1376.

[23] X. Yang, J. Wang, D. Song, B. Feng, and H. Ye, "A novel NLOS error compensation method based IMU for UWB indoor positioning system," *IEEE Sensors J.*, vol. 21, no. 9, pp. 11203–11212, May 2021.

[24] Z. Zeng, S. Liu, and L. Wang, "UWB/IMU integration approach with NLOS identification and mitigation," in *Proc. 52nd Annu. Conf. Inf. Sci. Syst.*, 2018, pp. 1–6.

[25] V. Barral, C. J. Escudero, J. A. García-Naya, and P. Suárez-Casal, "Environmental cross-validation of NLOS machine learning classification/mitigation with low-cost UWB positioning systems," *Sensors*, vol. 19, no. 24, Jan. 2019, Art. no. 5438.

[26] K. Bregar and M. Mohorčič, "Improving indoor localization using convolutional neural networks on computationally restricted devices," *IEEE Access*, vol. 6, pp. 17429–17441, 2018.

[27] S. Maranò, W. M. Gifford, H. Wymeersch, and M. Z. Win, "NLOS identification and mitigation for localization based on UWB experimental data," *IEEE J. Sel. Areas Commun.*, vol. 28, no. 7, pp. 1026–1035, Sep. 2010.

[28] K. Wen, K. Yu, and Y. Li, "NLOS identification and compensation for UWB ranging based on obstruction classification," in *Proc. 25th Eur. Signal Process. Conf.*, 2017, pp. 2704–2708.

[29] K. Yu, K. Wen, Y. Li, S. Zhang, and K. Zhang, "A novel NLOS mitigation algorithm for UWB localization in harsh indoor environments," *IEEE Trans. Veh. Technol.*, vol. 68, no. 1, pp. 686–699, Jan. 2019.

[30] B. Cao, S. Wang, S. Ge, and W. Liu, "Improving positioning accuracy of UWB in complicated underground NLOS scenario using calibration, VBUKF, and WCA," *IEEE Trans. Instrum. Meas.*, vol. 70, 2021, Art. no. 8501013.

[31] X. Yang, "NLOS mitigation for UWB localization based on sparse pseudo-input Gaussian process," *IEEE Sensors J.*, vol. 18, no. 10, pp. 4311–4316, May 2018.

[32] Z. Yin, X. Jiang, Z. Yang, N. Zhao, and Y. Chen, "WUB-IP: A high-precision UWB positioning scheme for indoor multiuser applications," *IEEE Syst. J.*, vol. 13, no. 1, pp. 279–288, Mar. 2019.

[33] Q. Zhang, D. Zhao, S. Zuo, T. Zhang, and D. Ma, "A low complexity NLOS error mitigation method in UWB localization," in *Proc. IEEE/CIC Int. Conf. Commun. China*, 2015, pp. 1–5.

[34] Q. Yang, Y. Zhang, W. Dai, and S. J. Pan, *Transfer Learning*. Cambridge, U.K.: Cambridge Univ. Press, 2020.

[35] B. Morawska, P. Lipinski, K. Lichy, and K. Adamkiewicz, "Transfer learning-based UWB indoor localization using MHT-MDC and clusterization-based sparse fingerprinting," *J. Comput. Sci.*, vol. 61, May 2022, Art. no. 101654.

[36] A. Morrison, N. Sokolova, and E. H. Eriksen, "Collaborative navigation for defence and emergency services," *Eur. J. Navigation*, vol. 13, no. 3, pp. 17–24, Dec. 2015.

[37] J. Rantakokko et al., "Accurate and reliable soldier and first responder indoor positioning: Multisensor systems and cooperative localization," *IEEE Wireless Commun.*, vol. 18, no. 2, pp. 10–18, Apr. 2011.

[38] L. Ruotsalainen, R. Guinness, S. Gröhn, L. Chen, M. Kirkko-Jaakkola, and H. Kuusniemi, "Situational awareness for tactical applications," in *Proc. Inst. Navigation GNSS*, 2016, pp. 1190–1198.

[39] N. Patwari, J. N. Ash, S. Kyperountas, A. O. Hero III, R. L. Moses, and N. S. Correal, "Locating the Nodes: Cooperative localization in wireless sensor networks," *IEEE Signal Process. Mag.*, vol. 22, no. 4, pp. 54–69, Jul. 2005.

[40] B. Zadrozny, "Learning and evaluating classifiers under sample selection bias," in *Proc. 21st Int. Conf. Mach. Learn.*, 2004, Art. no. 114.

[41] M. Mäkelä, J. Rantanen, J. Ilinca, M. Kirkko-Jaakkola, S. Kaasalainen, and L. Ruotsalainen, "Cooperative environment recognition utilizing UWB waveforms and CNNs," in *Proc. Eur. Navigation Conf.*, 2020, pp. 1–8.

[42] G. Kia, D. Plets, B. Van Herbruggen, E. De Poorter, and J. Talvitie, "Toward seamless localization: Situational awareness using UWB wearable systems and convolutional neural networks," *IEEE J. Indoor Seamless Positioning Navigation*, vol. 1, pp. 12–25, 2023.

[43] I. Goodfellow, Y. Bengio, and A. Courville, *Deep Learning*. Cambridge, MA, USA: MIT Press, 2016.

[44] R. Xia, Z. Pan, and F. Xu, "Instance weighting for domain adaptation via trading off sample selection bias and variance," in *Proc. 27th Int. Joint Conf. Artif. Intell.*, 2018, pp. 13–19.

[45] I. Skog, P. Handel, J.-O. Nilsson, and J. Rantakokko, "Zero-velocity detection an algorithm evaluation," *IEEE Trans. Biomed. Eng.*, vol. 57, no. 11, pp. 2657–2666, Nov. 2010.

[46] E. Foxlin, "Pedestrian tracking with shoe-mounted inertial sensors," *IEEE Comput. Graph. Appl.*, vol. 25, no. 6, pp. 38–46, Nov./Dec. 2005.

[47] S. Särkkä, *Bayesian Filtering and Smoothing*. Cambridge, U.K.: Cambridge Univ. Press, 2013.

[48] M. Mäkelä, M. Kirkko-Jaakkola, T. Hammarberg, T. Malkamäki, J. Rantanen, and S. Kaasalainen, "Cooperative heading estimation with von mises-fisher distribution and particle filtering," in *Proc. 25th Int. Conf. Inf. Fusion*, 2022, pp. 1–8.

[49] P. Strömbäck et al., "Foot-mounted inertial navigation and cooperative sensor fusion for indoor positioning," in *Proc. Int. Tech. Meeting Inst. Navigation*, 2014, pp. 89–98.

[50] F. Gustafsson, *Statistical Sensor Fusion*. Lund, Sweden: Studentlitteratur, 2010.

[51] J. Rantanen, L. Ruotsalainen, M. Kirkko-Jaakkola, and M. Mäkelä, "Height measurement in seamless indoor/outdoor infrastructure-free navigation," *IEEE Trans. Instrum. Meas.*, vol. 68, no. 4, pp. 1199–1209, Apr. 2019.